Damped Large Amplitude Transverse Oscillations in an EUV Solar Prominence

J. Hershaw[1], C. Foullon[1], V.M. Nakariakov[1,2] and E. Verwichte[1]

1: Centre for Fusion, Space and Astrophysics, University of Warwick, Coventry, UK. 2: Pulkovo Observatory, St. Petersburg, Russia.

1. Abstract

☼ We investigate two successive trains of large amplitude transverse oscillations in an arched EUV prominence, observed with SOHO/EIT on the North-East solar limb on 30 July 2005.

☼ The oscillatory trains are triggered by EUV global waves, associated with an X-class and a C-class flare occurring about 11 hours apart in the same remote active region.

☼ We use 195 Å images to compare oscillatory properties spatially, in the two legs of the prominence, at different heights, and between the two successively excited oscillatory trains.

☼ We discuss the results and their significance for shedding light on the effects of differing triggers, and for testing damping theories.

2. Event Overview

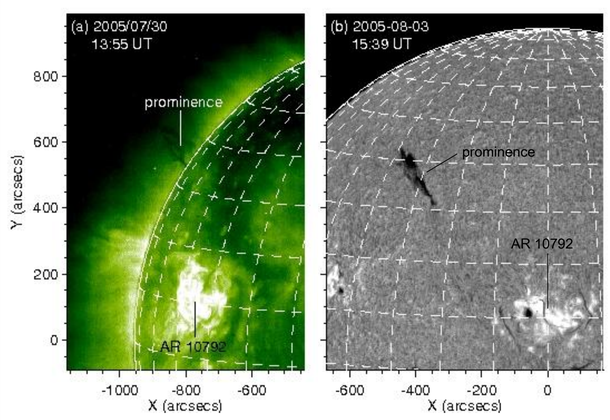

Fig. 1. (a) 195 Å intensity image from SOHO/EIT.
(b) H_α image 4 days later from Big Bear Solar Observatory

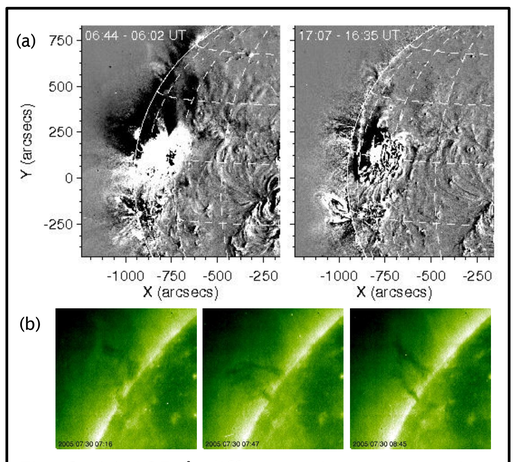

Fig. 2. (a) 195 Å difference images showing the two global EUV waves.
(b) 195 Å images of the 1st oscillatory train.

☼ **Two large flares on 30 July 2005**

- Both originating in active region 10792, detected by RHESSI and GOES-12
- 1st: X1.3 class flare peaking at 06:35 UT, with an associated type II radio burst
- 2nd: C8.9 class flare peaking at 17:07 UT, no radio burst detected

☼ **Each flare is followed by a global EUV wave**

- Intensity depletion is larger following the 1st wave, indicating a higher amplitude, see Fig. 2
- The shock occurring in the case of the 1st wave indicates a faster speed than that of the 2nd

☼ **Two trains of oscillations triggered in the prominence on the NE limb**

- Oscillatory behaviour starts at around 06:45 UT and continues over ~18 hours
- Observed by SOHO/EIT in 195 Å with a 12 min cadence, also 304 Å with a 6 hr cadence
- Horizontal displacements with respect to the solar surface, with periods of around 100 mins

3. Analysis

☼ **During the oscillatory phase the apparent height of the prominence varies with the rotation of the Sun**

- This can be modelled using a cosine curve (Foullon & Verwichte, 2006)

$$\frac{h(L)}{R_\odot} = \left(\frac{h_0}{R_\odot} + 1\right)\cos(L - L_0) - 1, \qquad (1)$$

  - L_0 = Carrington longitude of the prominence
  - L = Carrington longitude of the limb
  - h_0 = actual height above the solar surface
  - h = apparent height above the limb
- Using the 304/195 Å image ratio and considering an ROI encompassing the prominence, Fig. 3(a) is produced showing the maximum intensity versus height above the solar surface over Carrington longitude
- The observed apparent height of the prominence at each time-step, is identified using edge detection and fit to Eq. (1) giving:
- $h_0 = 0.170\ R_\odot$
- $L_0 = 27.5°$

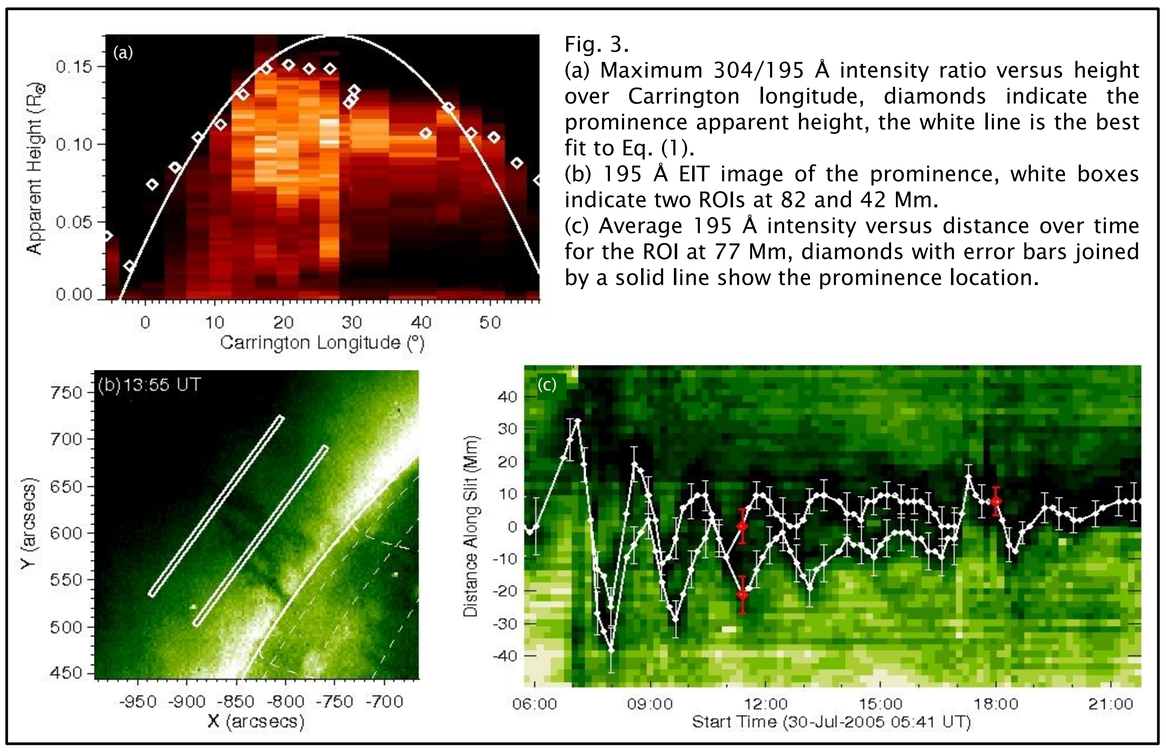

Fig. 3.
(a) Maximum 304/195 Å intensity ratio versus height over Carrington longitude, diamonds indicate the prominence apparent height, the white line is the best fit to Eq. (1).
(b) 195 Å EIT image of the prominence, white boxes indicate two ROIs at 82 and 42 Mm.
(c) Average 195 Å intensity versus distance over time for the ROI at 77 Mm, diamonds with error bars joined by a solid line show the prominence location.

☼ **Time series for the two prominence arch legs are extracted using Gaussian fitting on the 195 Å absorption features**

- 8 rectangular slits running parallel to the solar limb at different heights, are considered as shown on Fig. 3(b). These move with the apparent height profile of the prominence to account for solar rotation.
- The 195 Å intensity is averaged across the width of each slit, producing an image of intensity versus distance over time, such as Fig. 3(c).
- At each time-step, the intensity data is fitted to one (or two) Gaussian peak(s) with a second order polynomial background. The position of each prominence leg is identified by the Gaussian centroid, while the standard deviation of the Gaussian curve provides the error.

☼ **The time series are then fitted to a damped cosine curve**

$$x(t) - x_0(t) = \xi(t) = \xi_0 \cos\left(\frac{2\pi t}{P} - \phi\right)\exp\left(\frac{-t}{\tau}\right). \qquad (2)$$

- x = distance along slit
- $x_0 = a_0 + a_1 t$ = linear trend
- ξ = plane of sky (POS) displacement
- ξ_0 = initial POS displacement amplitude
- P = period
- ϕ = phase
- τ = decay time
- t = time

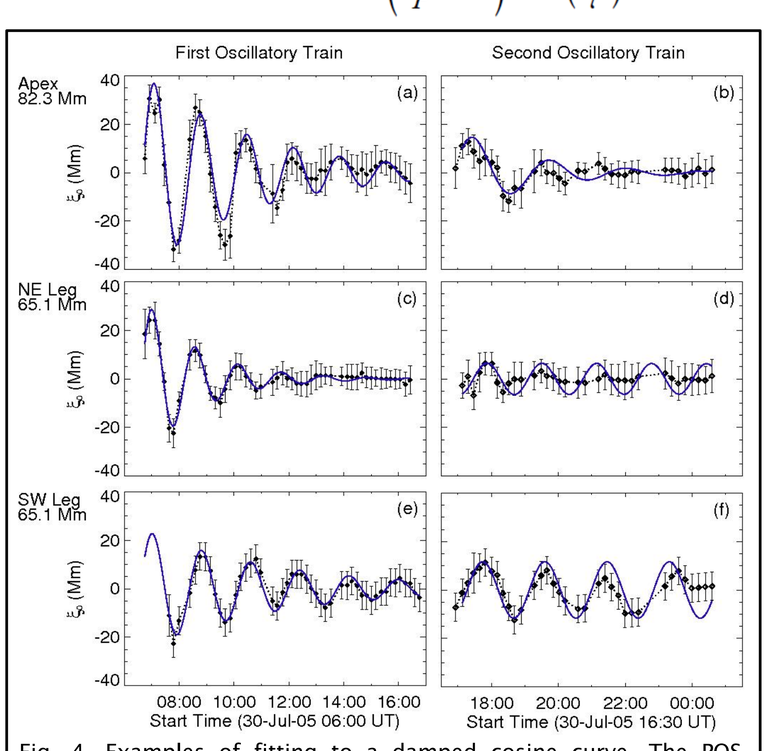

Fig. 4. Examples of fitting to a damped cosine curve. The POS displacements are shown as black diamonds with error bars joined by a dotted line, the blue line indicates the best fit to Eq. (2) using mean parameters from a randomisation technique.

- 'By-eye' estimates of position are used to obtain initial estimates of the parameters for a first fit to Eq. (2).
- Gaussian noise is added to each point to produce a randomised time series. This is fitted to Eq. (2), using the parameters from the first fit as initial estimates, with the linear trend now fixed. The process is repeated 500 times, giving a distribution of values for each parameter.
- Oscillation parameters are taken to be the mean values of the distribution, while their errors are given by the standard deviations.
- The initial transverse velocity amplitude $v(t)$ is estimated from the orientation of the prominence axis in Fig. 1(b).

4. Conclusions

☼ **Correspondence in kinetic energy between the flare, EUV global wave and prominence oscillation, for the two successive events**

- 1st flare has 14.6 times the energy of the 2nd
- 1st EUV wave has a larger amplitude and wave speed
- Amplitude at the apex is ~3x higher for the 1st oscillatory train than the 2nd, the kinetic energy is ~10x higher, see Fig. 5.(a)

☼ **Prominence exhibits a collective transverse oscillation, indicative of a global kink mode, to a first approximation**

- The period shown in Fig. 5.(b), is similar in both trains, with a global average of 99 ± 11 mins, suggesting a characteristic frequency as predicted by MHD
- During the first oscillatory train, the amplitude in Fig. 5.(a) increases with height, corresponding to the prominence oscillating as a whole with fixed footpoints
- Fig. 5.(c) shows that oscillations start approximately in phase between the two legs and regardless of height

☼ **Indications that the prominence oscillates as a collection of separate but interacting filamentary threads**

- A slight increase of period with height is apparent in Fig. 5.(b), suggesting the period of each thread may be affected by various factors which depend on height
- Periods in the NE leg are typically around 10% shorter than those in the SW leg.
- During the first oscillatory train, the velocity amplitudes in the SW leg are 10-15 km s^{-1} less than those in the NE leg, as seen in Fig. 5(a)

☼ **An approximately linear dependence of damping time upon period, consistent with resonant absorption as the damping mechanism**

- For resonant absorption, Ofman & Aschwanden (2002) assume a high density contrast and that the inhomogeneous layer thickness ∝ loop width, to obtain the scaling law $\tau \propto P$
- whereas for phase mixing they find $\tau \propto P^{4/3}$
- However, variation in the loop parameters may affect these scaling laws when applied to multiple events, due to variation in the loop parameters (Arregui et al. 2008)
- Measurements from this prominence alone, in Fig. 5(d), show a tendency towards a linear trend
- Combining our results with those of previously analysed kink mode coronal loop oscillations, we obtain the best fit to $\tau = cP^\alpha$, see Fig. 6, with
- $\alpha = 0.9 \pm 0.1$ = power law index
- $c = 1.6 \pm 0.2$ = constant
- The wide scattering of data points is likely a result of the expected variation in density contrast and layer thickness
- By extending the range of periods and damping times up to 2 decades, the influence of the varying parameters on the scaling is diminished

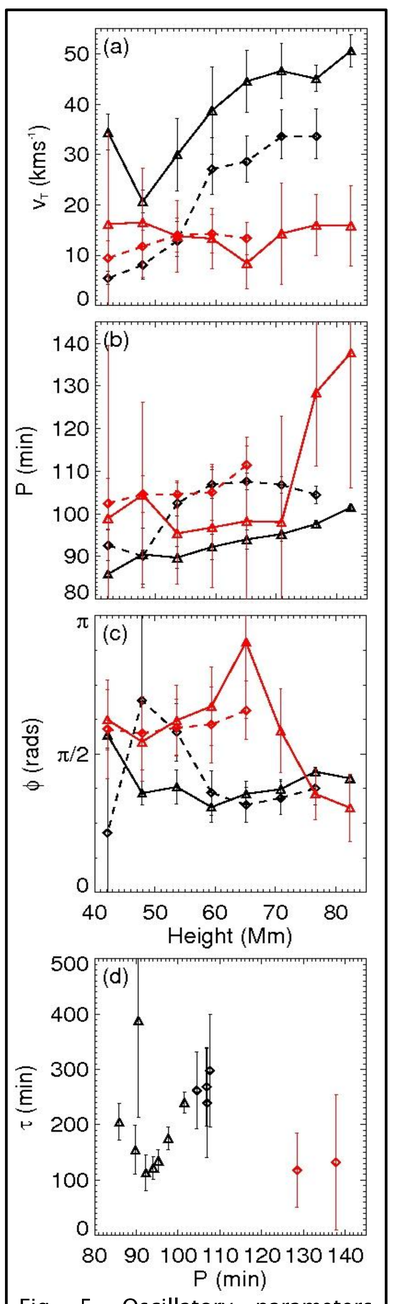

Fig. 5. Oscillatory parameters.
Black = first oscillatory train.
Red = second oscillatory train.
Triangles & solid line = NE leg.
Diamonds & dashed line = SW leg.

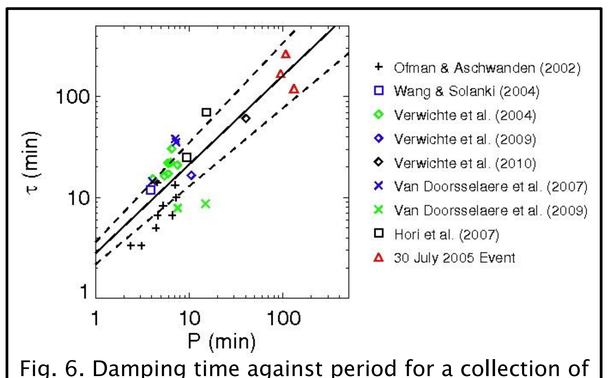

Fig. 6. Damping time against period for a collection of kink oscillations. Solid line is the best fit to $\tau = cP^\alpha$, with uncertainties indicated by dashed lines.

☼ **For references, see the forthcoming article: Hershaw et al. (2011)**